



Faculty of Applied Sciences - Department of Chemistry
Centre for Education and Research on Macromolecules
(CERM)

# DETERMINATION OF THE RELATIONSHIP BETWEEN FOAM MORPHOLOGY AND ELECTRICAL CONDUCTIVITY OF POLYMER/CARBON NANOTUBE NANOCOMPOSITE FOAMS

Dissertation presented by

**Minh-Phuong TRAN**

To obtain the grade of
Doctor in Science
Academic year 2013 - 2014

The present thesis has been supervised by the promoter
Dr. Christophe DEMTREMLEUR

This document presents the original results of the doctoral research carried out by TRAN Minh-Phuong, Chemist, M.Sc.

Université de Liège – Faculté des Sciences
Département de Chimie
Sart-Tilman, B6a, Allée de la Chimie
B-4000 Liège, Belgique
azianphuong@yahoo.com

**Jury members (February 20th, 2014)**

Professor Pierre DUYSINX…….President Jury
Dr. Christophe DETREMBLEUR……Promoter
Dr. Jean-Michel THOMASSIN……Secretary
Professor Christine JÉRÔME
Professor Isabelle HUYNEN
Professor Raquel VERDEJO
Research Engineer Sylvie GIRAULT

The research presented in this thesis was financially supported by Fund of ARC Project – N° 09/14-02 Bridging
From Imaging to Geometrical Modeling of Complex Micro Structured Materials: Bridging Computational Engineering and Material Science


**Pôle en Ingénierie Electrique (ELEN)**
**Université Catholique de Louvain**


Center for Applied
Technology in Microscopy (CATμ)


Montefiore Institute


Aérospatiale & Mécanique



**Faculty of Sciences – Department of Chemistry**

**REMERCIEMENT**

Je tiens tout d'abord à remercier mon directeur de thèse, Monsieur DETREMBLEUR Christophe, Directeur de Recherche du FNRS, qui m'a dirigé durant ce travail. Je suis reconnaissante envers lui pour ses encouragements, son enthousiasme et sa confiance. Je le remercie également de m'avoir donné l'opportunité d'assister à plusieurs congrès internationaux et de corriger mes publications internationales.

Je voudrais exprimer mes remerciements les plus sincères, mes profondes gratitudes et reconnaissances à THOMASSIN Jean-Michel, mon co-promoteur de recherche, pour m'avoir conseillée, encouragée et soutenue tout au long de mon travail avec beaucoup de patience et de disponibilité, et pour la confiance qu'il m'a accordée.

Je tiens à adresser mes remerciements à Madame JEROME Christine, Professeur Ordinaire, Directrice de Centre d'Education et de Recherche sur Macromolécules (CERM, Université de Liège), pour m'avoir accueillie dans son laboratoire.

J'adresse mes vifs remerciements aux Professeur Pierre DUYSINX, qui est mon Président Jury de thèse; Professeur Isabelle HUYNEN, Professeur Raquel VERDEJO, Ingénieur de recherche Sylvie GIRAULT d'avoir accepté d'être rapporteurs de ce travail et de m'avoir fait l'honneur de participer à ce jury de thèse.

J'adresse un grand merci à Monsieur Michael ALEXANDRE en tant que co-promoteur de ma thèse, qui m'a donné ses expériences précieuses dans le domaine de nanocomposites et aussi des conseils utiles à la caractérisation des propriétés de mousses. Tout mon grand merci à Monsieur Philippe LECOMPTE, de m'avoir enseigné la pratique de la RMN et donné des cours intéressant de RMN à l'état solide. J'adresse également un très grand merci à Martine DEJENEFFE et Valérie COLLARD, qui m'ont aidé à faire des belles images de SEM et TEM de mousses, qui m'ont montré les techniques de freeze-drying et qui m'ont donné de précieux conseils. Je remercie Charlotte DANNEMARK pour ses conseils utiles à faire la TGA et DSC. Je tiens à remercier Raphael RIVA pour m'avoir enseigné l'analyse de GPC et pour m'avoir aidé à résoudre les problèmes de connexion d'Internet au CERM.

Je remercie toutes mes collègues au CERM, en particulier à Bruno GRIGNARD pour m'avoir aidé à préparer les mousses dans $CO_2$ supercritiques et donné un coup de main à temps pour ouvrir les réacteurs trop serrés, et surtout pour tes conseils sincères dans la vie et l'amour. Je ne dois pas oublier à dire des remerciements à mon cher collègue Cédric BOYERE, qui a partagé le bureau avec moi pendant quatre ans. Durant le

temps de ce doctorat que je considère comme la période la plus heureuse dans ma jeunesse, nous avons eu beaucoup de discussions et de temps géniaux en participant aux activités variées au Labo, les sorties, les voyages à l'étranger, les blagues, les souris de rien, etc. Tout grand merci pour toi. Je souhaite adresser mes remerciements à Mathilde CHAMPEAU et Ji LIU, qui ont partagé l'espace commun dans notre petit bureau durant le temps de votre travail en Belgique, je tiens à remercier Ji pour le sentiment asiatique, pour les histoires de ton pays et du mien. Et Mathilde, je t'adresse un grand merci, je me souviendrai pour toujours de ta gentillesse, de ton sourire brillant, de ta confiance et aussi des secrets de filles que nous avons partagés.

Enfin, je tiens à remercier individuellement tous les membres du CERM et tous les étudiants qui y ont séjourné pour leur sympathie et leur accueil, grâce à qui j'ai pu effectuer ma thèse dans de très bonnes conditions et dans une ambiance chaleureuse. A côté de vous, mes amis, j'ai pu non seulement m'envoler sur des horizons scientifiques, mais aussi vivre une aventure intéressante de la vie en Belgique. A Enza ESPOSITO, Krystina, et Sophie BOULANGER de vos aides concernant les papiers administratifss et toutes les activités que vous avez bien organisées. À Antoine DEBUIGNE, je te remercie de tes conseils utiles à rédiger ma thèse. À Ian GERMAN de tes enseignements à bien prononcer les nomenclatures des substances chimiques en anglais, à Grégory CARTIGNY de ta force en m'aidant à ouvrir le tank d'azote liquide et aussi pour ton très bon humour, tes blagues très marrantes et des moments souriants que tu m'as apporté. À Farid OUHIB pour ces connaissances d'utiliser Soxhlet et pour tes aides à me ramener au Labo dans ta voiture dans les intempéries ou la grève de bus. À Anthony KERMAGORET de tes gentillesses et de nous sauver Cédric et moi avec tes biscuits lorsque nous travaillons tard le soir. À Martine et Jean-Mi encore une fois qui ont bien organisées les activités telles que le volley-ball, les sorties avec nos collègues, le kayak, le base-ball (auquel je joue pour la première fois en Belgique). Merci aux autres que je ne cite pas entièrement ici, à ceux qui m'ont aidé d'une façon discrète et silencieuse. A tous les nouveaux collègues; Laetitia, Kévin, Jérémy, Mathile 1èr, 2ème, 3 ème, Mirco, Daniela, Stéphanie, Stéphan, Sandro, etc; bon courage pour votre chemin scientifique.

Ce travail est le résultat d'étroites collaborations dans le cadre de l'Action Recherche Concertée (ARC) y compris cinq départements au sein de l'Université de Liège : Aerospace and Mechanical Engineering Departement – LTAS, Departement of Electrical Engineering and Compute Science (Institute Montefiore) – ACE, Centre for Educaton and Research of Macromolecules – CERM, Departement of Applied Chemistry – Laboratory of Chemical Engineering (LGC), Centre for Applied Technology in

Microscopy (CATμ). Je vous remercie vivement pour la collaboration efficace pendant ma thèse.

Je tiens à remercier vivement Monsieur Philippe VANDERBEMDEN et Monsieur Jean-François FAGNARD pour m'avoir permis de réaliser la majeure partie des expériences de mesure de la conductivité électrique dans leur laboratoire, pour m'avoir transmis de précieuses connaissances et pour m'avoir conseillée et guidée avec bienveillance.

Que serait la vie d'une doctorante sans amis? Tout d'abord, je tiens à remercier mes chers co-équipiers de tennis de table de Herstal, Alain DE GRAFE, Cédric LIBERT, Marine LEDUC, Florent DE GRAEF, Jules MELLIONS, Salvatore LIBERT, Patrick et les autres membres du club. Vous avez apporté une ambiance très familière, des moments inoubliables dans ma vie en jouant ensemble notre sport passionné. Grâce à vous, je ne me trouve plus toute seule ici. Les matches tendus, les sourires éclatants, les soirées, les victoires et aussi les défaites, vous étiez toujours à côté de moi.

Pour tous mes amis vietnamiens. Tout d'abord je voudrais dire mes remerciements spéciaux à PHÙNG Ngọc Dũng, NGUYỄN ĐĂNG Việt Linh, HỒ Đức An, LÊ TRẦN Hoàng Long, et NGUYỄN Quỳnh Oanh, vous êtes mes meilleurs amis pendant ces 4 ans de mon séjour à Liège. Je n'arrive pas à imaginer comment serait ma vie sans vos présences. Je garderai pour toujours dans mon cœur, les belles mémoires, les nostalgies de nos temps, les jours inoubliables quand nous étions très jeunes et bien profités de la vie. Des sincères remerciements destinés à anh Chính, chị Ánh, anh Hứa Cường, cô Bùi Kim Hải, anh Hữu Bình, anh Lâm-chị Hải, anh Long chị Hà, anh Nam chị Tú, anh Tuấn kiến trúc, chị Tiểu Lan, anh Tùng- chị Minh, chị Vân, Toàn, Dân – pour tous les voyages légendaires que nous avons faits ensemble. Pour toi, Ngọc-Đô, je t'adresse tous mes sentiments respectés et chaleureux pour ce que tu m'avais apportés pendant les jours les plus difficiles de ma vie. Et les autres amis, Đăng Khoa, Anh Vũ – deux amis enfantins, Hồng Khanh, Tứ Hải, Lê Vũ – les équipiers supers dans un groupe génial de ping-pong, que j'ai rencontré dans tous les quatre coins dans ce monde immense dans le passé, que je ne cite pas entièrement, dans cet ouvrage, mais qui reste à côté de moi à la façon silencieuse.

Par ailleurs, je remercie mes amis vietnamiens qui habitent partout en Europe, et aussi à Chị Hương -Hà Nội, toute la famille des Cocodies de Coudon – Toulon, en France. A Laetitia CICHY pour ta super gentillesse et des inoubliables fêtes de Noël en France avec ta grande famille. A Chung Di – Thanh Tùng aux USA, deux meilleurs amis dès mon enfance. A Thuý Anh en Australie, l'amie intime qui m'a toujours donné de bons conseils pour mon métier et aussi l'amour. A Ái Quang, à côté de toi, tu m'as apporté toujours de bons sens d'humour et tu as de grandes oreilles à bien m'écouter.

Au groupe de «  8 yêu » au Saigòn, Việt Nam, qui m'a supporté pendant des jours de jeunesse. A Cao Cường, tu es toujours des souvenirs sacrés, je me sens très heureuse d'être ton amie pendant 10 ans, super amitié!

A tous mes amis de notre classe légendaire A13, vous êtes toujours de supers camarades pendants 3 ans au lycée. Au groupe de DT, nous nous sommes souvent demandés à qui nous deviendrions dans l'avenir lorsque nous étions petits. En ce jour-là, la plupart de de nos rêves ont été réalises. Tout ce que je veux dire est que vous garderez une grande place dans ma nostalgie et des plus beaux moments que j'apprécie.

Je tiens à remercier vivement à Châu VO (Dow Europe GmbH, Switzerland) qui m'a aidée beaucoup pendant le temps de congrès internationaux que j'avais occasion d'y participer, et aussi de ses conseils précieux à mon travail scientifique.

*A Prince, grand merci à toi, mon amoureux! Tu es toujours à côté de moi et me soutiens par ton amour profond et ton humour exceptionnel. Je t'aime, mon cœur.*

*A ma famille, Bà Ngoại, Bà Nội, Dì Hà, Các Cô Chú, Thầy Cô, Anh chị em họ hàng thân thiết. Cám ơn những lời động viên, những tình cảm ấm áp dành cho Con.*

*Cám ơn Ba Mẹ vì vô vàn tình yêu thương, hy sinh để cho con nên người.*

*Cám ơn chị Nguyệt, người chị thân thiết và đồng hành với em trên mỗi bước đường em đi qua.*

*... I am grateful to my parents (Ba Hùng, Mẹ Thuỷ), my family for their endless love. I love you…*

*Especially for YOU!*

*Kính tặng Ba Mẹ!*

---

***"Share your knowledge. It is a way to achieve immortality"***
***— Dalai Lama XIV***

---

# Table of Contents

***Chapter 1, Chapter 3, Chpater 4, Chapter 5 can't be published now. Wait for publishing in journal.***

## Table of Contents

# INFLUENCE OF FOAM MORPHOLOGY OF MULTI-WALLED CARBON NANOTUBES/POLY (METHYL METHACRYLATE) NANOCOMPOSITES ON ELECTRICAL CONDUCTIVITY


## Abstract

*Polymer/multi-walled carbon nanotubes (PMMA/MWNTs) nanocomposites foams are widely investigated during the last decade thanks to their potential applications as electromagnetic interferences shielding (EMI) materials. Electrical conductivity of the nanocomposite is a key parameter for these applications. In the frame of this work, we aim at establishing relationships between the foams morphology and their electrical conductivity. We therefore first design nanocomposite foams of various morphologies using supercritical carbon dioxide ($scCO_2$) as physical foaming agent. The nanocomposites based on poly(methyl methacrylate) (PMMA) and different carbon nanotubes loadings are prepared by melt-mixing and foamed by $scCO_2$ in various conditions of pressure, temperature and soaking time. The influence of these foaming conditions on the morphology of the foams (volume expansion, pore size, cell density, cell-wall thickness) is discussed. After measuring the electrical conductivity of the foams, we establish structure/properties relationships that are essential for further optimizations of the materials for the targeted application.*


*Tran, M.-P., Detrembleur, C., Alexandre, M., Jerome, C., Thomassin, J.-M., Polymer,* ***2013****, 54, 3261-3270.*

*Chapter 2*

## I. Introduction

Foams are considered as microcellular foams when the cell density is greater than $10^9$ cells per $cm^3$ of solid polymer and the average cell diameter is in the order of 10 μm.[1] In recent decades, nanocomposite microcellular foams have attracted a great interest thanks to their high toughness, high stiffness, high thermal stability and low dielectric constant.[2, 3,4] In addition to their lightweight, microcellular foams have a great potential in many applications such as in aerospace, automotive, home construction, telecommunication, sporting equipment, insulation, food packaging and electromagnetic interference shielding (EMI shielding).[5]

Since their discovery by S. Iijima,[6] the helical microtubules of graphitic carbon, named carbon nanotubes (CNTs), became quickly a key figure in thousands of studies. In contrast to carbon black, CNTs show an exceptional combination of mechanical and electrical properties such as very high strength (100-300 GPa), high stiffness (elastic modulus can reach 1TPa),[7] high aspect ratio, high thermal and electrical conductivity.[8,9] Therefore, CNTs are widely used as conductive fillers within polymer matrices such as polypropylene (PP),[10,5] polyurethane (PU), [11] poly(pyrrole) (PPy),[12] polystyrene (PS),[13,14] polycaprolactone (PCL)[15,16] and polycarbonate (PC)[17,18] to cite only a few. However, CNTs usually appear as agglomerated bundles because of their high Van Der Waals interactions via the aromatic system on their tubular surface. Therefore, the dispersion method must be appropriately chosen to achieve good CNTs dispersion, a mandatory requirement for the achievement of good electrical conductivity and good mechanical reinforcement of the polymer matrix.

The combination of these two concepts, microcellular foams and carbon nanotubes are very promising for the design of materials for EMI shielding applications. Indeed, the dispersion of CNTs to a polymer matrix imparts it the required electrical conductivity that is essential for the interaction of the material with the electromagnetic radiation. The foaming of the nanocomposite ensures the preservation of a low dielectric constant that limits the reflection of EM radiation at the material interface. Indeed the reflectivity is proportional to the mismatch between the wave impedances for

the signal propagating into air and into the absorbing material, respectively. The introduction of air into these nanocomposites by the formation of foam therefore limits this mismatch and improves the EM absorption.[11] Foaming polymer/CNTs nanocomposites is therefore a route toward the formation of EMI absorbers.

Various foaming methods are reported in the scientific literature to form nanocomposite foams with pore size varying from nanometric to micrometric scale including: thermally induced phase separation (TIPS) process,[19, 20] chemical foaming agent (CFA),[21, 22] casting and leaching of physical foaming agents (nitrogen, carbon dioxide)[23]. Importantly, $CO_2$ is an important physical foaming agent because it is environmentally friendly, nontoxic, nonflammable, easily recyclable, abundant and cheap. Many researchers have used it for the foaming of different nanocomposites such as polymer/clay [24,25, 26] and polymer/CNTs.[16,27,28,29,30,31] In the latter, Thomassin *et al.*. has demonstrated the interest of foaming poly(ε-caprolactone)/CNTs nanocomposites for preparing EMI absorbers. Chen et al. studied the influence of the aspect ratio [29] and the surface modification [27] of CNTs on the foam morphology of poly(methyl methacrylate) (PMMA)/CNTs nanocomposites. They also investigated the compression properties [28] of the foams but did not consider the electrical conductivity of the foams *vs* their morphology.

In this work, we aim at designing a large panel of nanocomposites foams based on carbon nanotubes (CNTs) loaded poly(methyl methacrylate) (PMMA) using the supercritical carbon dioxide ($scCO_2$) technology. The ultimate goal is to establish important relationships between the foam morphology (cell density, pore size, cell density, cell-wall thickness) and their electrical conductivity.

## II. Experimental part

### II.1 Materials

Poly(methyl methacrylate), PMMA, was purchased at Lucite® Diakon® Frost (weight-average molecular weight Mw = 51600 g/mol, polydispersity Mw/Mn = 1.70) and used as received.

Multi-walled carbon nanotubes (MWNTs) thin (average outer diameter: 10nm, average length: 1.5 microns, surface area: 250-300 $m^2/g$, carbon purity 90%) were supplied by Nanocyl$^{TM}$, Belgium and produced by Catalytic Carbon Vapor Deposition (CCVD).

Carbon dioxide was purchased from Sigma® with purity 99.8%, 501298 cylinder 48L. $CO_2$ was introduced into the stainless steel vessel by syringe pump TELEDYNE ISCO Model 260D.

Different weight percentages of MWNTs were dispersed in poly(methyl methacrylate) (PMMA) by Brabender® Mixer 50E (Model 835205-002) Roller Slade twin-screws at 180$^{o}$C using 60 rotations per minute (rpm) during 5 minutes. The nanocomposites were then put into Hot Press (Fortune SRA100) at 200$^{o}$C for 5 minutes and mold into disk with a diameter of 12 mm and a thickness of 3.0 mm.

### II.2 Foaming of MWNTs/PMMA nanocomposites in scCO2

MWNTs/PMMA foams were prepared using a batch process. Three samples were separately placed into the stainless steel vessel. Subsequently, $CO_2$ was pressurized into the vessel by using syringe with high pressure-liquid pump to get the supercritical state of $CO_2$. When the required pressure was achieved, the system was kept at a given pressure and temperature during 16 hours to ensure the sufficient saturation's amount of $CO_2$ and to reach its thermodynamic solubility.[32] After the soaking time, a rapid depressurization (1-2 seconds) was applied. The vessel was then put immediately into a water/ice bath in order to stabilize the foams. Samples

with 1wt%, 2wt%, 4wt%, and 8wt% of MWNTs were used as starting materials for foaming.

## II.3 Characterizations

Nanocomposites samples were cut into thin films 60-70 nanometers by LEICA Microtome EM UC6 at ambient temperature. Subsequently, the dispersion of MWNTs in PMMA matrix was characterized by Transmission Electronic Microscopy (TEM) – Philips CM100 (100 kV, Canon Tungsten).

The foam structure was observed by scanning electron microscopy (SEM) using a JEOL JSM 840-A microscope after metallization with Pt (30 nm).

The gravimetric method was applied to study the quantity of absorbed and desorbed $CO_2$. The sample was weighed immediately after saturating the sample at a given pressure and temperature and rapid depressurization on a METTLER TOLEDO XS 204 balance (error of device: d = 0.1mg/1mg) at ambient temperature. The following formula was used to calculate the quantity of absorbed $CO_2$:

$$mCO_{2absorption} = \frac{(m_{after.soaking} - m_{initial})}{m_{initial}} * 100\% \qquad (1)$$

However, unavoidable fluid escapes from the samples during the time transport from taking off the vessel to balance. A more precise determination of the amount of absorbed $CO_2$ is obtained by measuring desorption of $CO_2$ as a function of time. If the Fickian diffusion is assumed, the initial part of the desorption curves in function of square root time is linear following equation 2.

$$\frac{M_{d,t}}{M_{gas,t=0}} = \frac{4}{l}\sqrt{\frac{Dd * td}{\pi}} \quad \textbf{(2)} \quad \text{While } M_{d,t} = M_{gas,t=0} - M_{gas,t} \ (*)$$

This formula relies on three following assumptions: (1) the diffusion coefficient is fluid concentration independent, (2) the concentration is

uniform throughout the sample, (3) the diffusion occurs exclusively in one direction, perpendicular to the sample surface (flat disk).[33]

This formula can be simplified (from equation 2 and (*)): $M_{gas,t} = M_{gas,t=0} - \frac{4}{l}\sqrt{\frac{Dd*td}{\pi}} M_{gas,t=0}$ (3) which allows us to determine the quantity of absorbed $CO_2$ at t = 0.

The morphology of the foamed nanocomposites was analyzed by the program ImageJ 1.45 using a running Macro to characterize the pore size, standard deviation pore size, the number of pores on a surface image, and pore size distribution. The presented results were calculated by the SEM's images of three different sites of foam and then the average value was determined. Cell-density was then obtained by the formula: [34]

$N_{cell} = \left(\frac{n.M^2}{A}\right)^{3/2} * \frac{p_{solid}}{p_{foam}}$ (4), where $N_{cell}$ is the number of cells in a volume unit (cell/$cm^3$), n is the number of cells in a 2-dimension (2D) SEM image, M is the magnification, A is the surface area of SEM ($cm^2$), $p_{solid}$ and $p_{foam}$ are solid and foams density, respectively.

The cell-wall thickness was estimated by $\delta = d\left(\frac{1}{\sqrt{1-\rho_{foam}/\rho_{solid}}} - 1\right)$ [35] (5), where δ is the cell-wall thickness (μm), d is the pore size and $\rho_{foam}/\rho_{solid}$ is the ratio of foam density and solid density.

The density of multi-walled carbon nanotubes can be calculated by equation 6: [36] $\rho_{CNTs} = \frac{\rho_g(d^2 - d_i^2)}{d^2}$ (6) where ρg is the density of fully dense graphite which is equal to 2.25g/cm3, d and di are outer diameter and inner diameter of carbon nanotube, respectively. The theory of percolation threshold is considered as a volumetric phenomenon. Therefore, by knowing the $\rho_{CNTs}$, the weight percentage of MWNTs can be now transformed into

vol% MWNTs in order to be coherent with the interpretation in the part of the electrical conductivity.

The electrical conductivities of MWNTs/PMMA foams were measured by the method of volume resistivity with KEITHLEY 617 PROGRAMABLE ELECTROMETER. The volume resistivity was measured by applying a voltage across the sample and measuring the resulting current. The resistivity is calculated from the geometry of the electrodes and the thickness of the sample. To ensure the good contact between electrodes and samples, two copper threads of electrodes (purchased from FILSSYNFLEX Thernko 300H DrADEN, d = 0.3mm, nominal resistance 0 Ohm at 20$^{o}$C) were stuck on the sample surfaces by silver paint (AGAR Scientific G3649 Electrodag 1415).

## III. Results and Discussion

### III.1 Dispersion of MWNTs in PMMA matrix

To be efficient, nanocomposites must exhibit an adequate dispersion of the nanofillers. However, MWNTs tend to entangle into bundles due to their high aspect ratio (the ratio between tubular length and diameter) and intensive π-π interactions between their constitutive aromatic systems. The term of "adequate-dispersion" has two different meanings: (i) the disentanglement of MWNTs bundles or agglomerates to give a uniform dispersion of individual MWNTs throughout the polymer matrix, and (ii) the preservation of enough MWNTs-MWNTs contacts to allow the transportation of electrons within the polymer matrix. In **Figure 1**, the TEM micrographs show that a homogenous dispersion of MWNTs in the PMMA matrix is achieved by simply mixing MWNTs with PMMA in an internal mixer at 200$^{o}$C during 5 minutes. The bundles are not observed anymore and MWNTs appear separately to each other's (**Figure 1 (b)** and **(c)**). The main problem of this dispersion method is that MWNTs are strongly cut, and thus shortened, by the high shear-force during melt-mixing. Their length varies from 50 to 200 nm (**Figure 1 (c)**). Therefore, longer mixing time will be unfavorable because a further decrease of the MWNTs length will occur that

is detrimental to the electrical conductivity and therefore to the EMI shielding performances.[37,38]

## III.2 Adsorption and desorption of CO2 in nanocomposites

In our study, $CO_2$ is used as a physical foaming agent. Therefore, the amount of $CO_2$ that is absorbed within the polymer samples plays a decisive role in the foaming process. Indeed, high amounts of absorbed $CO_2$ are expected to increase the number of nucleation sites inside the sample, and consequently the cell density. Therefore, a complete study of the different parameters that affect this $CO_2$ amount is first envisioned. The percentage of $CO_2$ in neat PMMA is slightly higher than in PMMA loaded by MWNTs (1wt% to 8wt%) because neat PMMA possesses ester chemical groups that has a great chemical affinity for $CO_2$.[39] As a result, the substitution of part of PMMA by CNTs decreases the total affinity of the samples for $CO_2$ and therefore slightly reduces its adsorption (**Figure 2**).

As an illustration, at 40°C, about 25wt% $CO_2$ is absorbed in PMMA loaded with 1wt% MWNTs while this amount drops to about 15wt% at 95°C (**Figure 2**). This trend is the same for all the samples whatever the MWNTs content. The decrease of $CO_2$ density, when the temperature increases at a given pressure, accounts for this observation.[40] A lower amount of $CO_2$ molecules are indeed available in the reactor.

The influence of the soaking time on the amount of absorbed $CO_2$ is then studied. A pressure of 200 bar and a temperature of 120°C were arbitrary selected to start these studies. Under these conditions, the amount of absorbed $CO_2$ is logically increased for longer soaking times, independently of the amount of nanofiller. Therefore, in the following experiments, the soaking time has been set to 16h in order to ensure a high amount of absorbed $CO_2$ (**Figure 3**).

Desorption coefficient (Dd) of $CO_2$ in the PMMA matrix (loaded or not with MWNTs) is then evaluated by weighting the amount of absorbed $CO_2$ *vs* desorption time, thus when the $CO_2$ absorbed sample is exposed to ambient atmosphere. By plotting the weight of absorbed $CO_2$ ($M_{gas,\,t}$) in

afunction of square root desorption time ( $\frac{M_{d,t}}{M_{gas,t=0}} = \frac{4}{l}\sqrt{\frac{Dd*td}{\pi}}$ (Equation 2)) (see in **Figure 4**) for the different samples, we can extract the diffusion coefficient of $CO_2$ in the nanocomposites from the plot slope.[33] Moreover, by extrapolating the plot at time zero, the weight of absorbed $CO_2$ at time zero is obtained. The amount of absorbed $CO_2$ is consistent with our previous observations: the neat PMMA shows a slightly higher quantity of absorbed $CO_2$ compared to MWNTs loaded PMMA matrices.

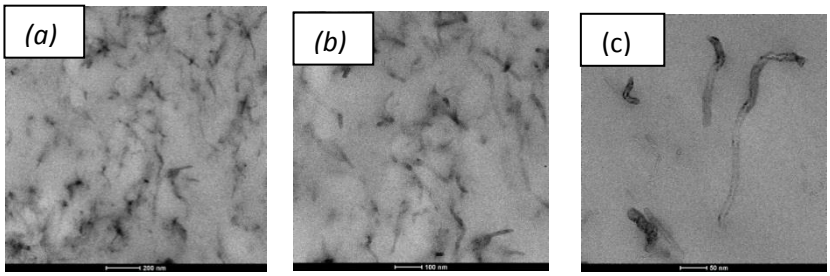


**Figure 1:** *TEM images of PMMA matrix loaded by 4wt% MWNTs, (a) magnification of 29000 (100nm sample thickness), (b) magnification of 50000 (100nm of sample thickness), (c) magnification of 100000 (80nm of sample thickness).*

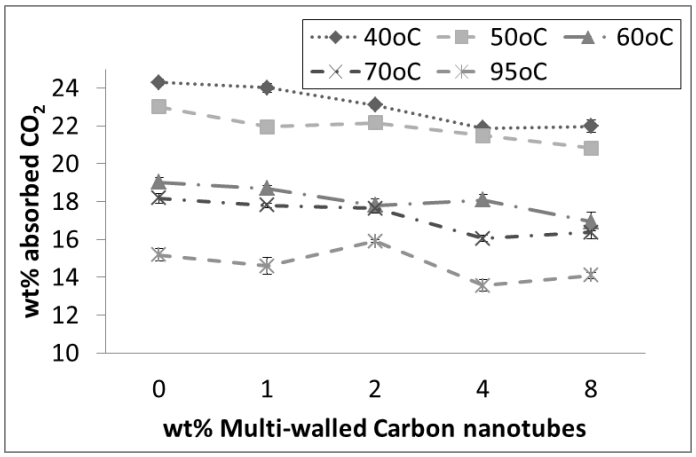


**Figure 2:** *Weight percentage of absorbed $CO_2$ in MWNTs/PMMA nanocomposite in function of the MWNTs loading and for different soaking temperatures (conditions: 180 bar, 16 h).*

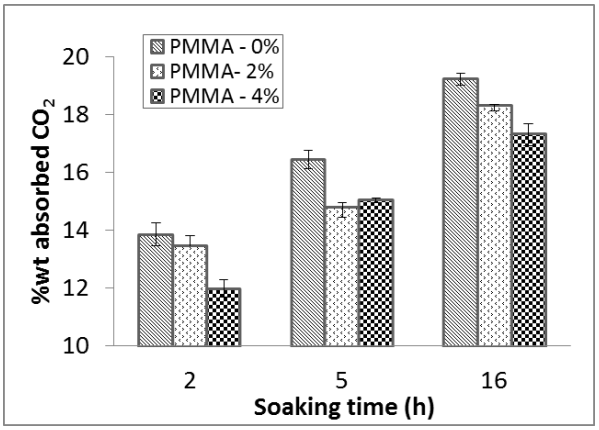


**Figure 3:** *Influence of soaking time on the weight percentage of $CO_2$ absorbed in PMMA matrices loaded with different amounts of MWNTs (conditions: 120°C, 200 bar).*

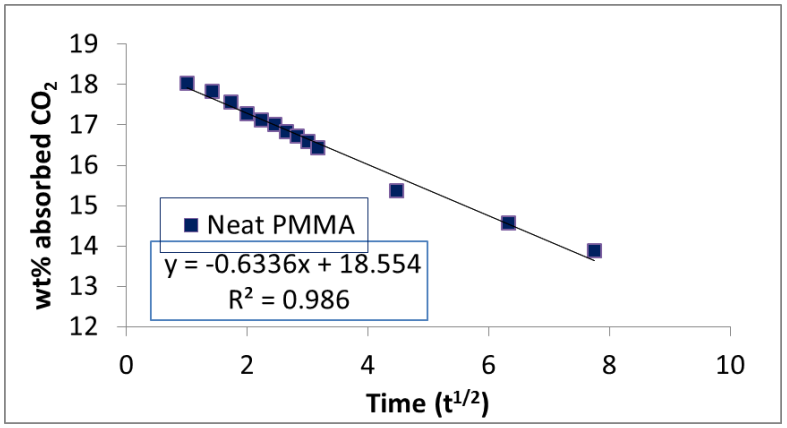


**Figure 4:** *Weight percentage of absorbed $CO_2$ in MWNTs/PMMA nanocomposite in function of square root time ($t^{1/2}$) (conditions: 120°C, 280 bar, 16h).*

The neat PMMA has also the highest diffusion rate (Dd = $2.23*10^{-2}$ $cm^2$/min) compared to 1.01 $10^{-2}$ $cm^2$/min and 6.75 $10^{-3}$ $cm^2$/min for PMMA loaded with 4wt% and 8wt% MWNTs, respectively (**Table 1**). A gradually decrease of the coefficient diffusion (Dd) is noted when increasing the content of MWNTs in PMMA matrix. The drop of diffusion coefficient (Dd) at higher content of MWNTs is explained by the fact that each MWNT can

be considered as a barricade to the diffusion of $CO_2$. The MWNTs network therefore increases the tortuosity of the system, slowing down the diffusion of $CO_2$. Similarly to clay of layered silicates, the platelets alignment enhances their effectiveness in gas barrier properties in creating a more tortuous path that prevents the gas molecules to cross the sample in a perpendicular direction to platelet orientation.[41,42,43]

**Table 1:** *Diffusion of $CO_2$ in MWNTs/PMMA nanocomposites after soaking at 120°C, 280 bar for16h.*

| Samples | %wt $M_{gas, t=0}$ | a (1) | L (2) (cm) | Dd ($cm^2$/min) |
|---|---|---|---|---|
| **Neat PMMA** | 18.6 | -0.634 | 0.3 | $2.23*10^{-2}$ |
| **PMMA – 2wt%CNTs** | 18.3 | -0.466 | 0.3 | $1.21*10^{-2}$ |
| **PMMA – 4wt%CNTs** | 18.1 | -0.427 | 0.3 | $1.01*10^{-2}$ |
| **PMMA – 8wt%CNTs** | 17.6 | -0.348 | 0.3 | $6.75*10^{-3}$ |

*(1) a was calculated from the slope of linear graph of desorption $-4.l^{-1}.(Dd.\pi^{-1})^{1/2}$, (2) L is the thickness of sample (cm); Dd is the diffusion coefficient ($cm^2$/min), $M_{gas, t=0}$ is the amount of $CO_2$ absorbed at time zero.*

### III.3 Influence of foaming conditions on foams morphology

#### III.3.1 Temperature

The influence of temperature on the foam parameters such as the pore size, the cell density, the volume expansion and the cell wall thickness is first considered.

For neat PMMA, the increase of temperature leads to the raise of pore size from 4.4 μm at 80°C to 10.5 μm at 120°C. The same trend is observed for PMMA containing MWNTs: from 0.8 μm at 80°C to 6.4 μm at 120°C **Figure 5 (a)**. It is important to note that although the pore size is slightly affected by the amount of MWNTs in the nanocomposite, foams of nanocomposites have smaller pore size than neat PMMA prepared under the same foaming conditions. **Figure 6** illustrates the SEM micrographs of neat PMMA and PMMA filled with 2, 4 and 8wt% of MWNTs foamed at 80°C,

100°C and 120°C. Although the increase of temperature favors the formation of larger pore size, the homogeneous morphology of closed-cells is maintained over this temperature range. Importantly, the foams morphology is also homogeneous at low MWNTs content as the result of the good MWNTs dispersion. In contrast Zeng *et al.*[44] who studied the foaming of PMMA/MWNTs prepared by the anti-solvent precipitation method, a bimodal cell size distribution was observed at low MWNTs content (1wt%). This observation is the result of the poor nanofillers dispersion and the presence of large MWNTs aggregates

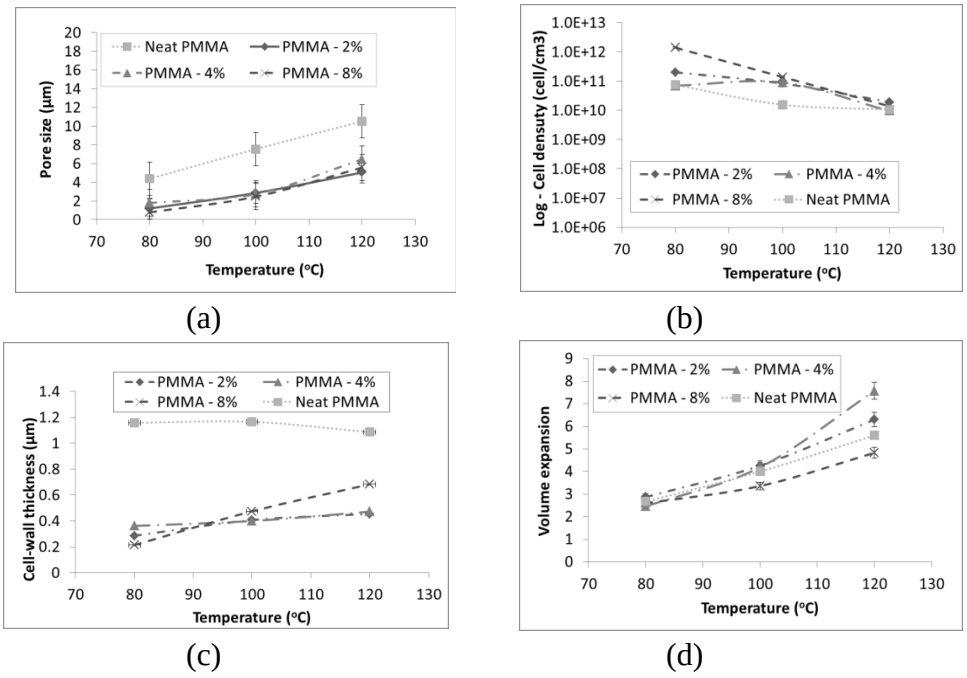


**Figure 5:** *Evolution of (a) pore size, (b ) cell density, (c) volume expansion, and (d) cell-wall thickness of PMMA foams loaded or not with MWNTs with the temperature (conditions:280 bar, 16h).*

. A good homogeneity of pentagonal cells was only achieved at higher concentration of MWNTs (≥ 2wt%). The increase of pore size with temperature observed in our nanocomposites is in line with the theory of nucleation and related articles: [2, 26,45] $N_1 = C_1 f_1 \exp\left(-\frac{\Delta G_{crit}^{*het}}{k_B T}\right)$ (7), where $N_1$

is the number of nuclei generated per $cm^3$, $f_1$ is the frequency factor of gas molecules joining the nucleus, $C_1$ is the concentration of heterogeneous sites, $k_B$ is the Boltzmann constant, and $\Delta G^*_{crit}$ is the work of forming a critical nucleus.

Adversely to the pore size, the cell density decreases with the foaming temperature for both neat PMMA and the nanocomposites (**Figure 5 (b)**). For instance, the cell density of foams (PMMA/8wt% MWNTs) decreases from $1.39 \times 10^{12}$ cells/$cm^3$ at 80°C to $1.38 \times 10^{10}$ cells/$cm^3$ at 120°C. The neat PMMA also shows the same trend with the cell density that decreases from $2.8 \times 10^{10}$ to $1.9 \times 10^{9}$ (cells/$cm^3$) by increasing the temperature from 80°C to 120°C. The decrease of the cell density with the temperature increase is in agreement with the theory of nucleation [46,47]

$$N_1 = C_1 f_1 \exp\left(-\frac{\Delta G^{*het}_{crit}}{k_B T}\right)$$

The $CO_2$ density decreases when increasing the temperature, which lowers the $f_1$ value, consequently decreasing the cell density.

Another important characteristic of the foam is the volume expansion compared to the starting un-foamed material (**Figure 5 (c)**). Similarly to the pore size, the volume expansion steadily increases with the foaming temperature. This increase follows the same trend whatever the MWNTs content. At 80°C, the volume expansion is about 2.6, while at 120°C, the highest volume expansion is 7.5 for the nanocomposite containing 4wt% MWNTs. Higher amounts of MWNTs do not affect further the volume expansion. Indeed the volume expansion is directly related to two main factors: pore size and number of nucleation sites. An increase of these characteristics will obviously be in line with an increase in volume expansion. Therefore, when MWNTs are incorporated into the polymer matrix, these nanofillers are acting as nucleating agents. The cell density and volume expansion are thus increased when the amount of MWNTs is increased. However, at high nanofiller loading (8wt%), too many heterogeneous sites lead to a competitive nucleation of embryos, resulting in the coalescence of lateral cells.

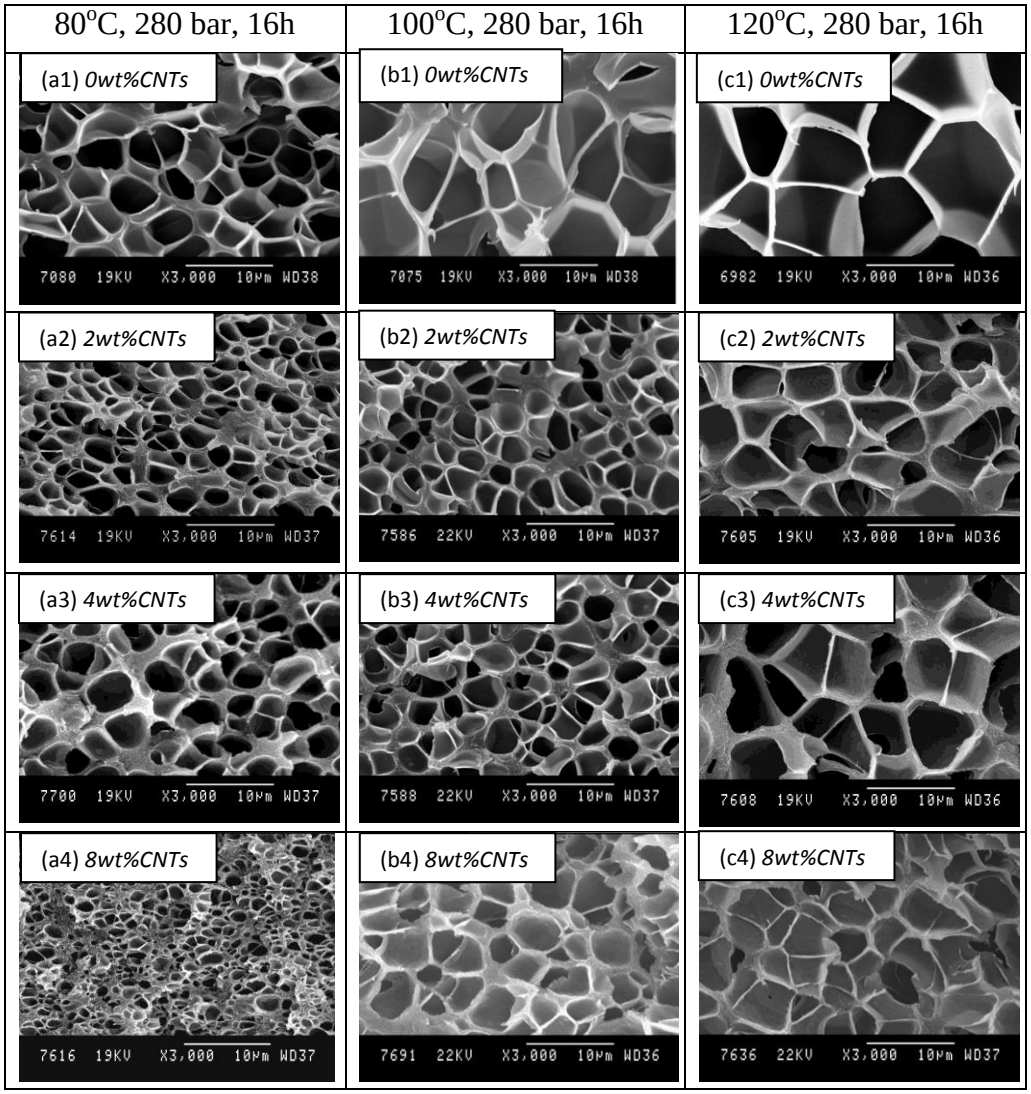


**Figure 6**: *SEM micrographs of PMMA foams prepared at different temperatures and various MWNTs loadings: (a) foaming at 80°C; (b) foaming at 100°C; (c) foaming at 120°C. Conditions: 280 bar, 16h.*

Finally, the influence of the temperature on cell-wall thickness is investigated. As shown in **Figure 5 (d)**, it can be seen that the cell-wall thickness for neat PMMA slightly decreases when increasing the temperature from 100°C to 120°C. The cell-wall thickness of PMMA filled CNTs is much lower in direct relation with smaller pore size. A slight increase with

the temperature is observed which is more pronounced when the CNTs content is very high (8wt%) due to smaller increase in volume expansion with the temperature in this case.

### III.3.2 Pressure

The influence of pressure on foam morphology is studied by keeping the temperature around the glass transition temperature ($T_g$) of PMMA ($120^oC$). As evidenced in **Figure 7 (a)** and **Figure 8**, an increase of pressure from 150 to 280 bar induces a considerable decrease of the cell size for both neat PMMA and PMMA loaded with MWNTs, while uniform and homogenous cells are maintained over the whole pressure range. For neat PMMA, the pore size decreases from 29.4 to 12.2 μm when increasing the pressure from 150 to 200 bar. Similarly, a significant decrease of the pore size was observed for PMMA loaded with 2 and 4wt% of MWNTs in the range of 150 to 200 bar. The reduction of pore size becomes less important upon further increase of the pressure. The cell-wall thickness of the nanocomposite foams is also reduced when the pressure is increased but in a much less extent than for neat PMMA (**Figure 8 (d)**). The phenomenon of decreasing the cell-wall thickness by increasing the pressure can be attributed to the decrease of both the pore size and volume expansion of foams.

In contrast to the pore size, a significant increase of cell density was observed when the pressure increases from 150 to 280 bar. For neat PMMA, the cell density increases from $1.07 \times 10^8$ cell/$cm^3$ at 150 bar to a value of $1.9 \times 10^9$ cell/$cm^3$ at 280 bar. A maximum of cell density is observed at 250 bar for PMMA samples filled with 4wt% and 8wt%MWNTs corresponding to $1.9 \times 10^{10}$cell/$cm^3$ and $6.6 \times 10^{10}$ cell/$cm^3$, respectively. The decrease of cell density when the pressure is further increase is due to the coalescence of lateral cells, which decreases the total number of individual cells.[48]

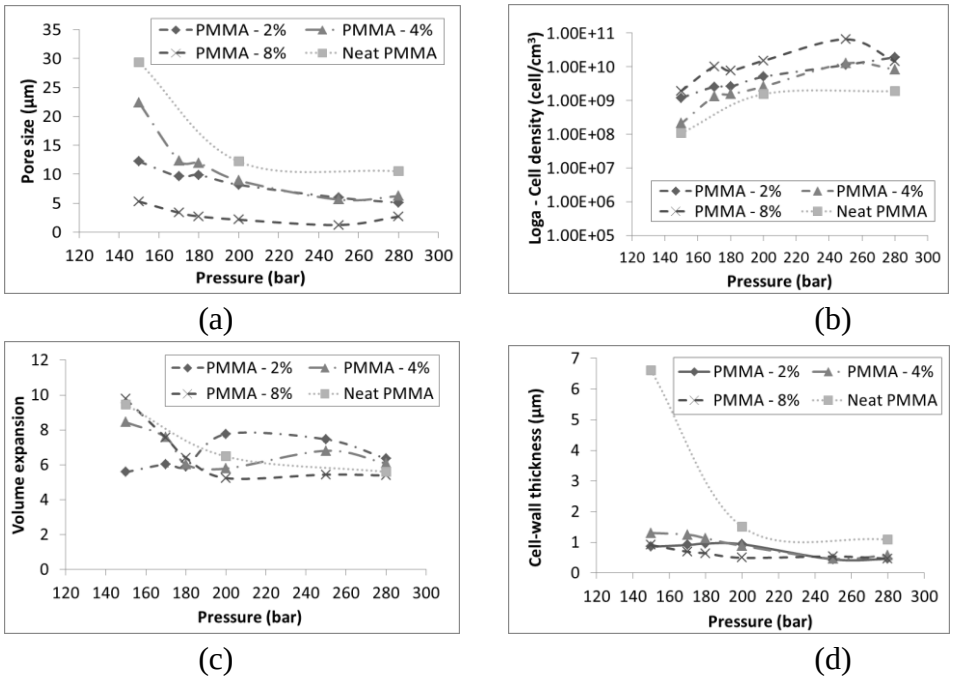


**Figure 7:** *Evolution of (a) pore size, (b ) cell density, (c) volume expansion, and (d) cell-wall thickness of PMMA foams loaded or not with MWNTs with the pressure (conditions:120°C, 16h).*

Generally, the cell density of the neat PMMA foam is smaller than the cell density of the PMMA filled CNTs.[44] It can be assumed that the different nucleation mechanisms, homogeneous in neat PMMA and heterogeneous in the nanocomposites, are responsible for this observation and are in agreement with Lee *et al.*[45] and with the nucleation theory. When the same foaming conditions are used for both samples (neat PMMA and PMMA loaded with MWNTs), the nanofiller is acting as heterogeneous nucleating agent in the nanocomposites, thus increasing the cell density compared to neat PMMA. The volume expansion of neat PMMA continuously decreases with the applied pressure from 9.4 at 150 bar to 5.6 at 280 bar (**Figure 7 (c)**). In the same tendency, the volume expansion varies around 6-7 when the polymer is filled with 2 and 4wt% of MWNTs. It is slightly lower for PMMA loaded with 8wt% MWNTs due to the high viscosity of the nanocomposite that limits the foam expansion.

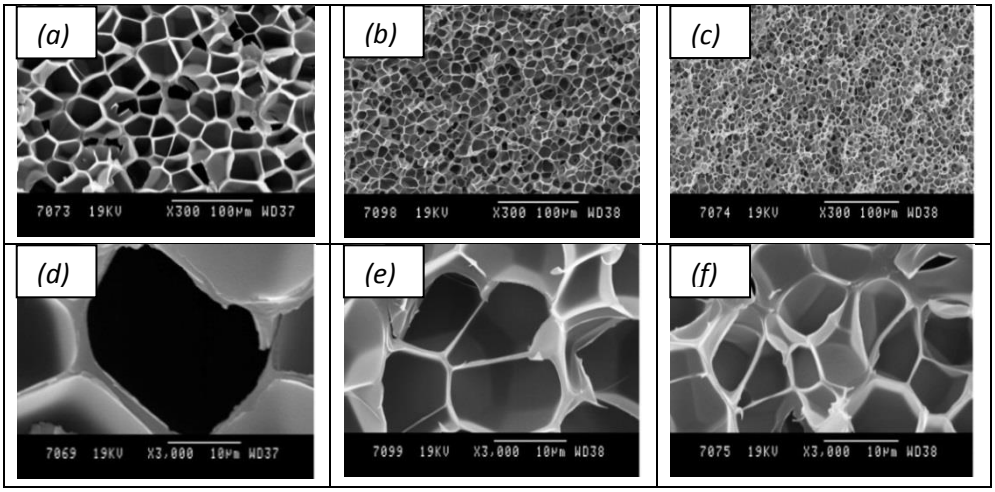


**Figure 8:** *SEM micrographs of PMMA foams prepared at different pressures: (i) SEM's images with magnification X300 (a)150 bar (b)200 bar, (c)280 bar; ii) SEM's images with magnification X3000 (d) 150 bar, (e) 200 bar, (f) 280 bar.*

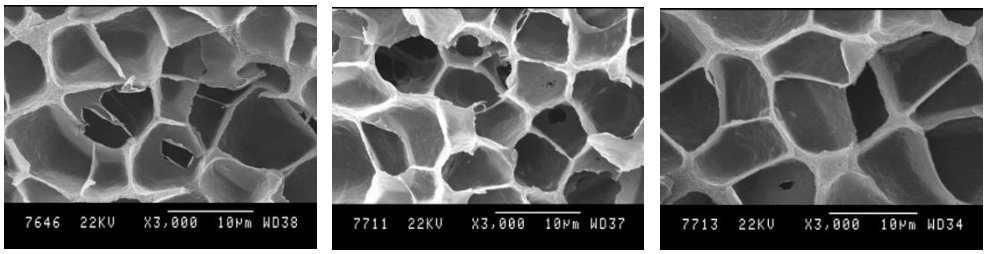


*150 bar* *170 bar* *180 bar*

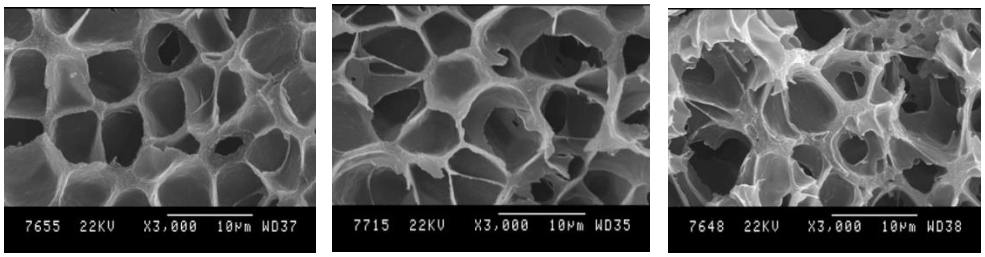


*200 bar* *250 bar* *280 bar*

**Figure 9:** *SEM micrographs of PMMA foams loaded with 8wt% MWNTs prepared at different pressures. Conditions: 120°C, 16h.*

A further increase of applied pressure over 280 bar is not favorable because it leads to heterogeneous foams as exemplified in **Figure 9** for PMMA filled with 8wt% MWNTs. Coalescence of lateral cells seems to occur that contributes to the formation of interconnected cells.

### III.4 Electrical conductivity

The electrical conductivity of PMMA/MWNTs solid samples is first investigated **Figure 10**. As expected, the increase of the amount of MWNTs in the PMMA matrix leads to the sharp raise of conductivity from 8.95 x $10^{-5}$ S/m at 0.49 vol% MWNTs to 311.5 S/m at 5.56 vol% MWNTs in the matrix. At this stage, it has to be noted that since the electrical measurements are performed on a given volume of sample, the electrical conductivities of the samples are compared for MWNTs loaded samples (foamed or non-foamed) with a MWNT content expressed in vol%.

In the case of foamed samples, the electrical conductivities also strongly depend on the content of the conductive nanofiller Figure 10. Importantly, for the same MWNT content, foamed nanocomposites present a much higher conductivity compared to solid ones. For instance, a conductivity of 1.7 S/m is measured for the foams containing 0.69 vol% MWNTs compared to less than 0.02 S/m for the solid sample with the same nanofiller content. A lower percolation threshold is therefore expected for the foams.

$$\sigma \alpha (p - p_c)^t \quad \text{for } p>p_c \qquad (8)$$

The value of this percolation threshold $p_c$ is found by the scaling theory in which the conductivity varies in function of $\log(p - p_c)$; in which $p$ is the concentration of MWNTs and $p_c$ is the critical concentration of MWNTs at percolation threshold. The exponent $t$ is identical and independent of the concentration of conductive charge, and $t$ depends only on the dimension of the matrix (2D or 3D) with the values typically around 1.3 and 2.0 for two and three dimensions, respectively.[49] As evidenced in **Figure 11**, the best fit of the conductivity corresponding to the scaling theory gives a percolation threshold $p_c$ at 0.29 vol% MWNTs for the foams and an

exponent t = 2.1. In the case of the solid samples, an increase of three orders of magnitude (8.95 x $10^{-5}$ S/m at 0.49 vol% MWNTs to 1.56 x $10^{-2}$ S/m at 0.69 vol% MWNTs) was observed. Therefore, the value of electrical percolation threshold of solid PMMA is located between 0.49 and 0.69 vol% MWNTs. In comparison to PMMA solid, PMMA foams has lower electrical percolation threshold.

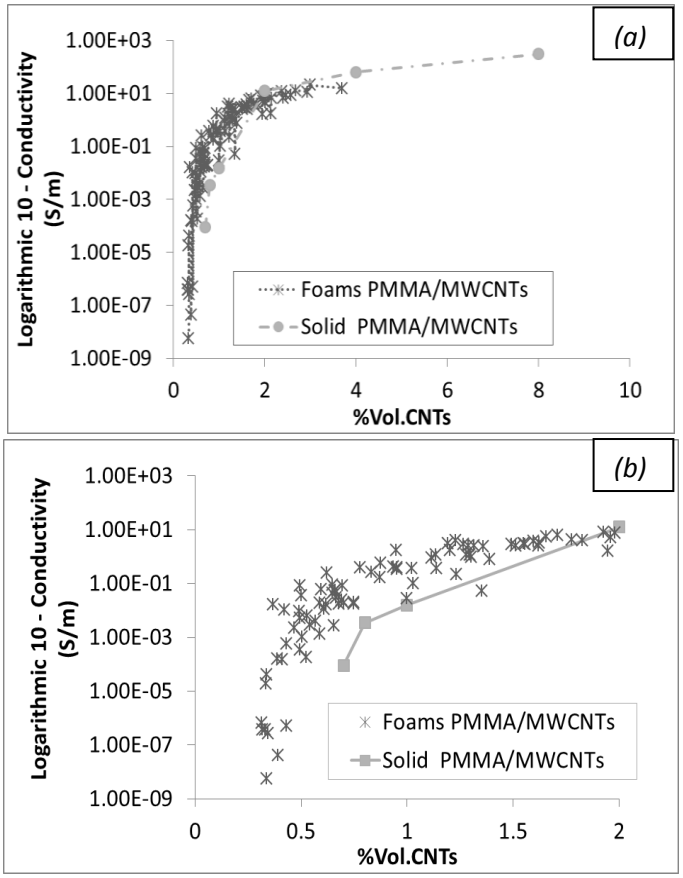


**Figure 10:** *Electrical conductivity of PMMA/MWNTs nanocomposites foamed and not foamed in function of MWNTs content: (a) full range of MWNTs content and (b) zoom of the 0 – 2 vol% MWNTs range.*

The important difference in percolation threshold between foamed and un-foamed nanocomposites is explained by the selective localization of MWNTs inside the cell walls of the foam that induces a significant decrease

of the average distance between them as illustrated in **Figure 12**. Thus, an effective electrical network can be formed at lower MWNTs concentration compared to solid sample. It is in agreement with the work of Thomassin *et al.*[16]. Increased volume expansion (for the same MWNTs loading) leads therefore to higher conductivities as shown in **Figure 13**.

To highlight further the influence of the morphological parameters of the foam on the electrical conductivity, foams with similar contents of MWNTs but different pore sizes, cell densities and cell wall thicknesses are selected and compared **Figure 14**.

At low vol% of MWNTs (0.42 and 0.66 vol%), a strong decrease of conductivity is recorded when increasing the pore size (**Figure 14 (a)**) while the conductivity significantly raises with the increase in cell density (**Figure 14 (b)**). This phenomenon can be explained by the theory developed by Xu *et al.*[50] Upon foaming, MWNTs preferentially localize in the cell-struts, the inter-connecting point of three surrounding bubbles. Consequently, the electrical conductivity is strongly depending on the ability of the foams to keep an electrical network between these struts. The increase in pore size results in increasing the distance between adjacent struts and then increases the probability to break the conductive network.

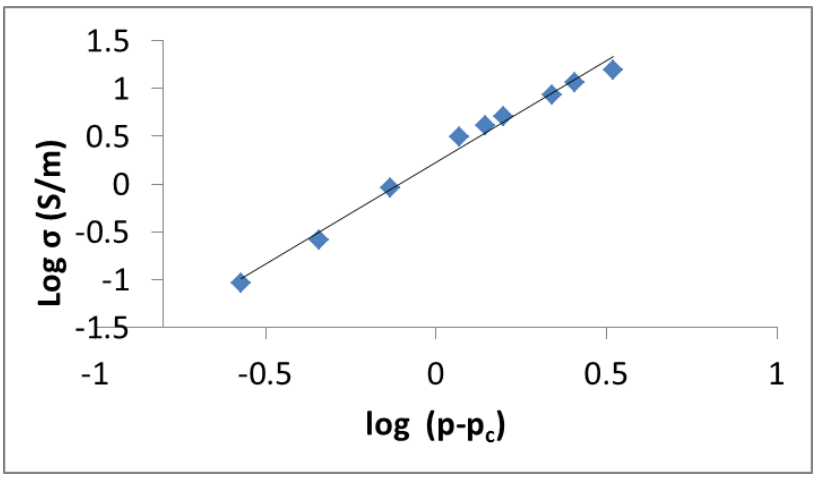


**Figure 11:** *The fitted curve of conductivity to scaling theory when logσ (conductivity) was plotted against log* $(p - p_c)$ *with* $p_c = 0.29\%$ *and* $t = 2.1$.

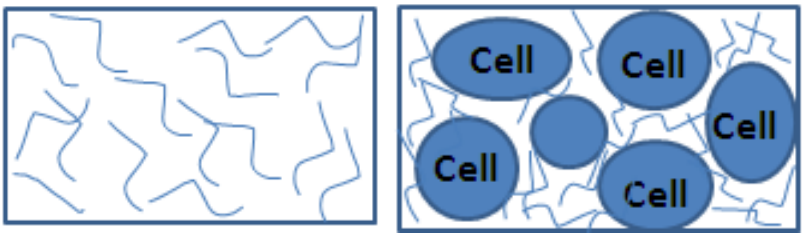


**Figure 12:** *Distribution of MWNTs in nanocomposties (a) in unfoamed nanocomposites, (b) in foamed nanocomposites.*

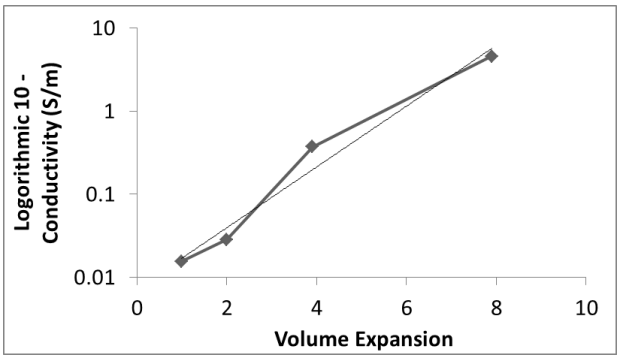


**Figure 13:** *Dependence of the volume expansion on the electrical conductivity for a PMMA/MWNTs foam containing 1 vol% MWNTs.*

A sharp decrease of conductivity is also observed when increasing the cell-wall thickness. The advantage to reduce the cell wall thickness comes from the fact that MWNTs are more confined in thin cell wall therefore increasing the probability of effective MWNTs-MWNTs contacts that are essential for the establishment of an electrical network. However, the cell wall thickness cannot be decreased indefinitely due to the risk of breaking this network by the cell-wall rupture.

At higher content of MWNTs (1.3vol%), the conductivity [51] is high and also decreasing with the pore size but in a more marginal way. The same trend is observed for cell-wall thickness.[52] At this MWNTs loading, the preservation of the electrical network between the struts is more probable, and the effect of the morphological parameter on the conductive properties is lower.

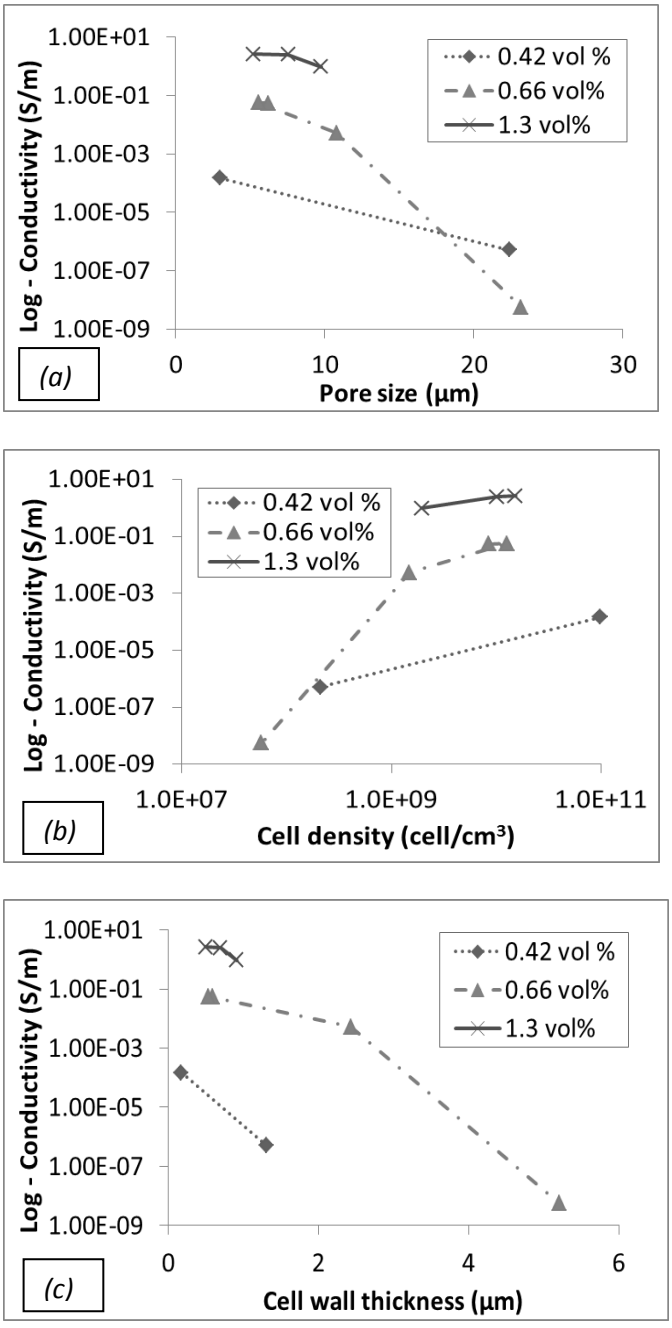


**Figure 14:** *Evolution of electrical conductivity of PMMA/MWNTs foams of different MWNTs loadings with the (a) pore size,(b) cell density, (c) cell-wall thickness.*

**Table 2:** *Comparison of the electrical conductivity of PMMA/MWNTs nanocomposites foamed and non-foamed with different MWNTs loadings*

| Sample solid vol%CNTs | Conductivity (S/m)-Solid | Foams vol% CNTs | Conductivity (S/m)-Foams | Foaming conditions |
|---|---|---|---|---|
| **0.21** | X (>200G.Ohm) | **0.21** | $6.78 \times 10^{-7}$ | 120°C, 280 bar, 16h |
| **0.35** | X (>200G.Ohm) | **0.35** | $1.02 \times 10^{-3}$ | 120°C, 150 bar, 16h |
| **0.49** | $8.95 \times 10^{-5}$ | **0.49** | $1.93 \times 10^{-2}$ | 120°C, 200 bar, 16h |
| **0.56** | $3.44 \times 10^{-3}$ | **0.54** | 0.38 | 100°C, 150 bar, 16h |
| **0.69** | $1.56 \times 10^{-2}$ | **0.66** | 1.69 | 110°C, 280 bar, 16h |
| **1.39** | 12.7 | **1.40** | 4.58 | 100°C, 150 bar, 16h |

## IV. Conclusion

Conductive homogeneous microcellular foams of poly(methyl methacrylate)/carbon nanotubes nanocomposites were prepared by using supercritical carbon dioxide as a physical foaming agent. The effect of the foaming conditions (pressure and soaking temperature) on the foams morphology (pore size, cell density, volume expansion cell-wall thickness) was first investigated in order to produce a large variety of foams with different morphologies. Then their electrical conductivity was studied and compared to unfoamed samples with the same volume content of the conductive nanofiller. A lower percolation threshold was observed for the foams as the result of the selective localization of CNTs inside the cell walls of the foams that induces a significant decrease of the average distance between them. The systematic measurement of the electrical conductivity of the different foams then allowed establishing important foam morphology/conductivity relationships. The electrical conductivity continuously increased with the volume expansion as the result of the

selective localization of the CNTs inside the cell wall. Increasing the air fraction in the foam shortens the distance between CNTs at a given CNTs volume content. The increase of the cell density also raised the electrical conductivity while increasing the pore size or the cell-wall thickness had the opposite effect. From this work, it can therefore be concluded that foams with a high electrical conductivity can be achieved when high volume expansion, small pore size, high cell density, and thin cell-wall thickness are targeted. This study states the guidelines to tailor foamed materials with high electrical conductivity.

## V. Acknowledgements

The authors are grateful to the National Fund for Scientific Research, Region Wallonia, Belgian Science Policy Office" in the frame of the Interuniversity Attraction Pole Program (PAI VI/27). This research was also supported by the French Community of Belgium and the Wallonia-Europe Academia in the frame of the "Action de Recherche Concertée" (ARC project). C.D. and I.H. are Research Directors by F.R.S.-FNRS.

## V.I References

1. Kumar, V., *Prog. Rubber Plast. Technol.*, **1993**, 9, 54-70.

2. Collias, D.I., Baird, D.G.,Borggreve, R.J.M., *Polymer*, **1994**, 35, 3978-83.

3. Tomasko, D.L., Li, H., Liu, D., Han, X., Wingert, M.J., Lee, L.J., et al., *Ind. Eng. Chem. Res.*, **2003**, 42, 6431-6456.

4. Kumar, V., *Cell. Polym.*, **1993**, 12, 207-23.

5. Thomassin, J.-M., Huynen, I., Jerome, R.,Detrembleur, C., *Polymer*, **2010**, 51, 115-121.

6. Iijima, S., *Nature (London)*, **1991**, 354, 56-8.

7. Demczyk, B.G., Wang, Y.M., Cumings, J., Hetman, M., Han, W., Zettl, A., et al., *Mater. Sci. Eng., A*, **2002**, A334, 173-178.

8. Tans, S.J., Devoret, M.H., Groeneveld, R.J.A.,Dekker, C., *Nature (London)*, **1998**, 394, 761-764.

9. Hamada, N., Sawada, S.,Oshiyama, A., *Phys. Rev. Lett.*, **1992**, 68, 1579-81.

10. Lee, S.H., Cho, E.N.R., Jeon, S.H.,Youn, J.R., *Carbon*, **2007**, 45, 2810-2822.

11. Huynen, I., Quievy, N., Bailly, C., Bollen, P., Detrembleur, C., Eggermont, S., et al., *Acta Mater.*, **2011**, 59, 3255-3266.

12. Tellakula, R.A., Varadan, V.K., Shami, T.C.,Mathur, G.N., *Smart Mater. Struct.*, **2004**, 13, 1040-1044.

13. Li, B., Wu, Q., Zhou, N.,Shi, B., *Int. J. Polym. Mater.*, **2011**, 60, 51-61.

14. Fragneaud, B., Masenelli-Varlot, K., Gonzalez-Montiel, A., Terrones, M.,Cavaille, J.Y., *Compos. Sci. Technol.*, **2008**, 68, 3265-3271.

15. Pan, L., Pei, X., He, R., Wan, Q.,Wang, J., *Colloids Surf., B*, **2012**, 93, 226-234.

16. Thomassin, J.-M., Pagnoulle, C., Bednarz, L., Huynen, I., Jerome, R.,Detrembleur, C., *J. Mater. Chem.*, **2008**, 18, 792-796.

17. Hornbostel, B., Poetschke, P., Kotz, J.,Roth, S., *Phys. Status Solidi B*, **2006**, 243, 3445-3451.

18. Li, C., Zhao, Q., Deng, H., Chen, C., Wang, K., Zhang, Q., et al., *Polym. Int.*, **2011**, 60, 1629-1637.

19. Tanaka, T., Eguchi, S., Saitoh, H., Taniguchi, M.,Lloyd, D.R., *Desalination*, **2008**, 234, 175-183.

20. Li, S., Wang, K.,Li, M., *J. Macromol. Sci., Part B: Phys.*, **2010**, 49, 897-919.

21. Youssef, H.A., Senna, M.M.,Eyssa, H.M., *J. Polym. Res.*, **2007**, 14, 351-357.

22. Matuana, L.M., Faruk, O.,Diaz, C.A., *Bioresour. Technol.*, **2009**, 100, 5947-5954.

23. Jacobs, L.J.M., Kemmere, M.F.,Keurentjes, J.T.F., *Green Chem.*, **2008**, 10, 731-738.

24. Taki, K., Yanagimoto, T., Funami, E., Okamoto, M.,Ohshima, M., *Polym. Eng. Sci.*, **2004**, 44, 1004-1011.

25. Urbanczyk, L., Calberg, C., Detrembleur, C., Jerome, C.,Alexandre, M., *Polymer*, **2010**, 51, 3520-3531.

26. Zeng, C., Han, X., Lee, L.J., Koelling, K.W.,Tomasko, D.L., *Adv. Mater. (Weinheim, Ger.)*, **2003**, 15, 1743-1747.

27. Chen, L., Goren, B.K., Ozisik, R.,Schadler, L.S., *Compos. Sci. Technol.*, **2012**, 72, 190-196.

28. Chen, L., Schadler, L.S.,Ozisik, R., *Polymer*, **2011**, 52, 2899-2909.

29. Chen, L., Ozisik, R.,Schadler, L.S., *Polymer*, **2010**, 51, 2368-2375.

30. Chen, L., Schadler, L.S.,Ozisik, R., *PMSE Prepr.*, **2008**, 99, 642-643.

31. Athanasopoulos, N., Baltopoulos, A., Matzakou, M., Vavouliotis, A.,Kostopoulos, V., *Polym. Compos.*, **2012**, 33, 1302-1312.

32. Goel, S.K.,Beckman, E.J., *Cell. Polym.*, **1993**, 12, 251-74.

33. Pantoula, M.,Panayiotou, C., *J. Supercrit. Fluids*, **2006**, 37, 254-262.

34. Kumar, V.,Suh, N.P., *Polym. Eng. Sci.*, **1990**, 30, 1323-9.

35. Okamoto, M., Nam, P.H., Maiti, P., Kotaka, T., Nakayama, T., Takada, M., et al., *Nano Lett.*, **2001**, 1, 503-505.

36. Thostenson, E.T.,Chou, T.-W., *J. Phys. D: Appl. Phys.*, **2003**, 36, 573-582.

37. Lee, B.O., Woo, W.J., Park, H.S., Hahm, H.S., Wu, J.P.,Kim, M.S., *J. Mater. Sci.*, **2002**, 37, 1839-1843.

38. Thomassin, J.-M., Lou, X., Pagnoulle, C., Saib, A., Bednarz, L., Huynen, I., et al., *J. Phys. Chem. C*, **2007**, 111, 11186-11192.

39. Mawson, S., Johnston, K.P., Combes, J.R.,DeSimone, J.M., *Macromolecules*, **1995**, 28, 3182-91.

40. Friedmann, S.J., *Elements (Chantilly, VA, U. S.)*, **2007**, 3, 179-184.

41. Bharadwaj, R.K., *Macromolecules*, **2001**, 34, 9189-9192.

42. Osman, M.A., Mittal, V.,Lusti, H.R., *Macromol. Rapid Commun.*, **2004**, 25, 1145-1149.

43. Thellen, C., Orroth, C., Froio, D., Ziegler, D., Lucciarini, J., Farrell, R., et al., *Polymer*, **2005**, 46, 11716-11727.

44. Zeng, C., Hossieny, N., Zhang, C.,Wang, B., *Polymer*, **2010**, 51, 655-664.

45. Lee, L.J., Zeng, C., Cao, X., Han, X., Shen, J.,Xu, G., *Compos. Sci. Technol.*, **2005**, 65, 2344-2363.

46. Fletcher, N.H., *J. Chem. Phys.*, **1958**, 29, 572-6.

47. Shen, J., Zeng, C.,Lee, L.J., *Polymer*, **2005**, 46, 5218-5224.

48. Zhai, W., Wang, H., Yu, J., Dong, J.,He, J., *Polym. Eng. Sci.*, **2008**, 48, 1312-1321.

49. Sandler, J.K.W., Kirk, J.E., Kinloch, I.A., Shaffer, M.S.P.,Windle, A.H., *Polymer*, **2003**, 44, 5893-5899.

50. Xu, X.-B., Li, Z.-M., Shi, L., Bian, X.-C.,Xiang, Z.-D., *Small*, **2007**, 3, 408-411.